Annealing C_{60}^+: Synthesis of Fullerenes and Large Carbon Rings

Joanna Hunter, James Fye, Martin F. Jarrold

Laser vaporization of graphite generates C_{60}^+ cluster ions that are fullerenes and a mixture of roughly planar polycyclic polyyne ring isomers. Experimental studies of the annealing of the non-fullerene C_{60}^+ ions indicate that they can be converted (in the gas phase) into the fullerene and an isomer that appears to be a large monocyclic ring. Some fragmentation is associated with conversion to the fullerene geometry, but the majority of the non-fullerene C_{60}^+ isomers are cleanly converted into an intact fullerene. The emergence of the monocyclic ring (as the clusters are annealed) suggests that this is a relatively stable nonspheroidal form of these all carbon molecules. The estimated activation energies for the observed structural interconversions are relatively low, suggesting that these processes may play an important role in the synthesis of spheroidal fullerenes.

How highly symmetric fullerenes spontaneously nucleate in a superheated carbon vapor remains unresolved. Smalley, Kroto, Curl, and their co-workers (*1*) originally envisioned an icospiral nucleation process where the dangling bonds at the edge of graphitic fragments naturally induced curvature by closing-up to form pentagonal rings. Although direct formation of fullerenes from graphitic fragments has been ruled out by $^{12}C/^{13}C$ isotope studies (*2*), other groups have proposed that fullerenes grow predominantly from specific building blocks such as C_2 or C_{10} units (*3–6*). A common feature of these models is the notion that fullerenes must grow by some well-defined route with intermediates that can clearly be identified as fullerene precursors. However, some recent results challenge this assumption. McElvaney and co-workers have recently presented evidence indicating that fullerenes which result from laser desorption of *cyclo*-$C_{18}(CO)_6$, *cyclo*-$C_{24}(CO)_8$, and *cyclo*-$C_{30}(CO)_{10}$ are generated by direct coalescence of large polyyne rings (*7*). We have addressed the issue of how fullerenes assemble from a different perspective. We have examined the structural interconversions of non-fullerene C_{60}^+ ions to determine whether they can be converted into fullerenes.

The experiments were performed with a tandem quadrupole drift tube apparatus (*8*). C_{60}^+ ions, generated by pulsed laser vaporization of graphite in a helium buffer gas and size-selected with a quadrupole mass spectrometer, are injected at various energies into a drift tube containing ~5 torr of helium. The cluster ions experience a transient heating cycle as they enter the drift tube and undergo many collisions with the buffer gas. At high injection energies, the clusters may be heated to the point that they anneal or even dissociate (*9*). After the clusters' kinetic energy is thermalized, they are rapidly cooled by further collisions with the buffer gas. The clusters' structure is then probed by measuring their mobility as they travel through the 7.6-cm drift tube under the influence of a weak electric field. The mobility is effectively a measure of the cluster ions' size (*10*). Thus the compact fullerenes can easily be separated from the less compact planar isomers. The mobility measurements are performed by injecting a 50-μs pulse of cluster ions into the drift tube and recording their arrival time distribution at the detector. Any fragmentation that occurs at high injection energies is monitored by recording the mass spectrum of the cluster ions that exit the drift tube.

The arrival time distribution recorded for C_{60}^+ (see Fig. 1) shows two components. These can be assigned on the basis of the previous work of Bowers and co-workers (*10*), who have performed mobility measurements for unannealed carbon cluster ions. The sharp, faster moving component at ~800 μs is due to the fullerene. The broad, slower moving component at longer times can be assigned to a mixture of unresolved roughly planar polycyclic polyyne ring isomers. The distribution shown in Fig. 1 was recorded with an injection energy of 100 eV. With injection energies up to ~100 eV, no significant annealing or dissociation of the C_{60}^+ clusters occurs, so the relative abundances obtained from these results reflect the isomer distribution generated by the source. Integration of the areas under the two components in Fig. 1 shows that the combined relative abundance of the planar polycyclic ring isomers (50 to 60%) is slightly greater than that of the fullerene. Although we have not performed an exhaustive study, these relative abundances appear to be only slightly sensitive to the source conditions used.

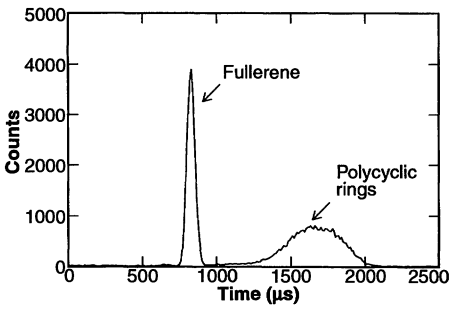

Fig. 1. Arrival time distribution for C_{60}^+ ions generated by pulsed laser vaporization of graphite; an injection energy of 100 eV was used.

If the injection energy is increased, the clusters can be excited to the point where they anneal or dissociate as they enter the drift tube (*9*). Arrival time distributions recorded for C_{60}^+ at several injection energies (Fig. 2) illustrate the changes that occur as the clusters anneal. As the injection energy is increased, the broad component centered at ~1700 μs gradually disappears, a sharp component grows in at ~1950 μs, and the relative abundance of the fullerene at ~800 μs increases. We have performed similar, although less detailed, studies for a range of smaller clusters and found that the mobility of the sharp component that grows in at ~1950 μs can be correlated almost exactly with the monocyclic ring isomers of smaller clusters first observed by Bowers and co-workers (*11*). The large size of the 60-atom monocyclic ring compared to the fullerene is illustrated in Fig. 3. In the results shown in

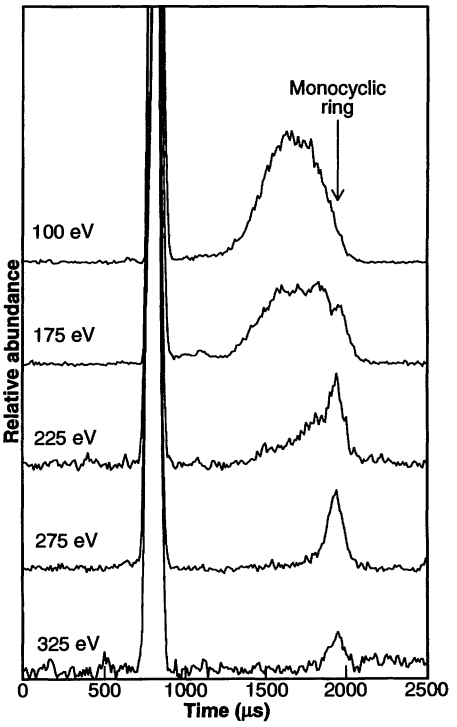

Fig. 2. Arrival time distributions recorded for C_{60}^+ ions with injection energies of 100, 175, 225, 275, and 325 eV.

Department of Chemistry, Northwestern University, Evanston, IL 60208.

Fig. 2, the monocyclic ring first becomes apparent at an injection energy of 175 eV. At this injection energy, there is another poorly resolved feature at slightly shorter times (~1800 μs). This feature, which is much more evident in our results for smaller clusters, can be assigned to a bicyclic ring (two fused polyyne rings) (*10*). As the injection energy is increased up to 275 eV, only two isomers remain in significant abundance: the fullerene and the feature assigned to the monocyclic ring. Ultimately, at the highest injection energies the monocyclic ring also disappears, leaving only the fullerene. We have compared the measured peak profiles for the fullerene and the monocyclic ring (at high injection energies) with those predicted by solution of the transport equation for ions in the drift tube (*12*). Both peaks can be fit by assuming that they consist of only a single component. However, we cannot rule out the possibility that one or both of these peaks consist of a number of isomers with similar shapes. For example, it is unlikely that we would be able to separate icosahedral C_{60}^+ from fullerene isomers that disobey the isolated pentagon rule.

In Fig. 4A the relative abundances of the C_{60}^+ fullerene, the monocyclic ring, and the polycyclic ring isomers are plotted against injection energy. These results are an average of three independent data sets. In addition to the changes that are illustrated in Fig. 2, a significant fraction of the C_{60}^+ ions dissociate as the injection energy is raised above 100 eV. The fraction of surviving C_{60}^+ ions is also shown plotted in Fig. 4A. At low injection energies, the observed product ions result from sequential loss of C_2 units to give species such as C_{58}^+ and C_{56}^+. The arrival time distribution for C_{58}^+ derived from the dissociation of C_{60}^+ is shown in Fig. 5. The single sharp component at ~800 μs indicates that the C_{58}^+ product ions are predominantly fullerenes, as are all of the fragments resulting from the loss of C_2 units. The relative abundance of these fullerene fragments is plotted against the injection energy in Fig. 4B. Direct dissociation of fullerene C_{60}^+ requires injection energies significantly greater than used here, and it appears from Fig. 4 that the fullerene fragments originate from the polycyclic ring isomers. Approximately one-half of the polycyclic rings anneal into an intact C_{60}^+ fullerene and about one-third fragment. The polycyclic rings probably anneal before they fragment, with the highly exothermic annealing process driving the subsequent fragmentation of the fullerene. The evidence to support this notion is primarily the observed fragmentation processes: loss of C_2 is the characteristic dissociation pathway of the fullerenes (*13, 14*). As the injection energy is raised above 250 eV, the relative abundance of the fullerene fragments remains approximately constant as the average number of C_2 units lost by the fullerene fragments continues to increase slightly. This observation suggests that the intact fullerene and fullerene fragments result from polycyclic ring isomers with substantially different stabilities: the more stable polycyclic rings resulting in the intact fullerene, and the less stable ones leading to fullerene fragments.

The relative abundance of the monocyclic ring reaches ~10% for injection energies of ~250 eV and then declines as the injection energy is raised further (see Fig. 4). At these high injection energies, a second group of products emerges, which are labeled as the ring fragments in Fig. 4B. These products range from C_{22}^+ to C_{46}^+ and show intensity variations with a periodicity of four. The relative abundances of the individual product ions are low, which impeded measurements of their arrival time distributions. However, analogous measurements for smaller clusters (where these fragments are much more abundant) suggest that these product ions are monocyclic rings. The observed periodicity of four is thus presumably related to aromatic stabilization of monocyclic polyyne rings with $4n + 2$ atoms. Dissociation into two roughly equal-sized monocyclic rings is probably the lowest energy dissociation pathway of the large monocyclic rings. The remarkable resilience of the large monocyclic ring suggests that this is a relatively stable nonspheroidal form of these all-carbon molecules. Although the appearance of the ring fragments is roughly correlated with the disappearance of the monocyclic ring, it appears from the results shown in Fig. 4 that only a fraction of the rings dissociate, the balance annealing into an intact fullerene. In contrast, for slightly smaller clusters (less than ~50 atoms), we find that fragmentation dominates.

In order to determine whether the structural interconversions reported here can play a role in fullerene synthesis, it is necessary to estimate their activation energies. Activation energies were determined from the fragmentation and annealing thresholds by using a modified impulsive collision model to estimate the internal energy of the injected clusters (*8, 9*), along with RRKM (Rice, Ramsperger, Kassel, and Marcus) theory (*15*) to model the statistical aspects of the dissociation and annealing of the excited C_{60}^+ ions [the RRKM model used here is essentially iden-

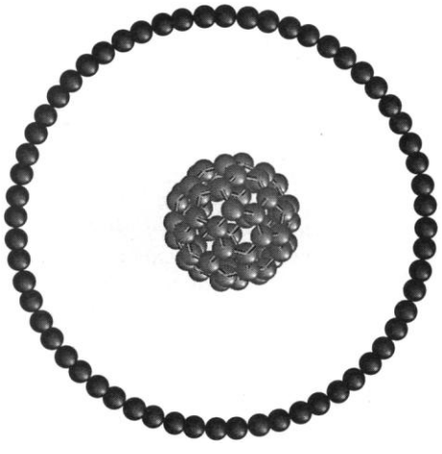

Fig. 3. Comparison of the monocyclic ring and fullerene geometries for a 60-atom carbon cluster.

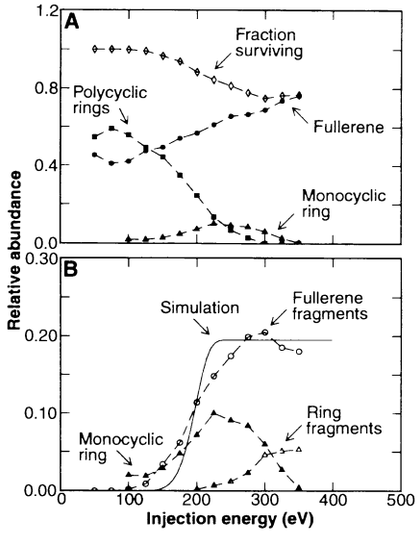

Fig. 4. (**A**) The relative abundances of the polycyclic ring isomers, the feature assigned to a monocyclic ring, and the intact fullerene plotted against the injection energy. The fraction of C_{60}^+ ions (all isomers) that survive injection is also shown. (**B**) The relative abundance of the fullerene fragments and the ring fragments plotted against injection energy (the relative abundance of the monocyclic ring is also shown). The solid line is the result of a simulation described in the text.

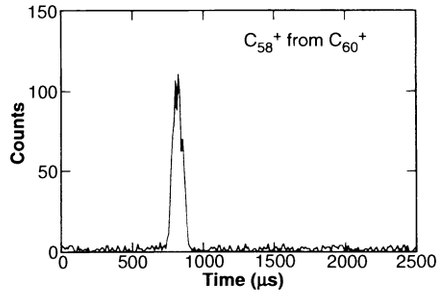

Fig. 5. The arrival time distribution recorded for C_{58}^+ ions resulting from the dissociation of the polycyclic ring isomers of C_{60}^+ at an injection energy of 250 eV. The single feature at ~800 μs is due to the fullerene.

tical to that used in several recent studies of the dissociation of C_{60} and C_{60}^+ (*16*)]. As a test of the model used to estimate the internal energy of the injected clusters, we used this method to determine dissociation energies for some of the smaller carbon clusters and found them to be in reasonable agreement with the values recently reported by Anderson and co-workers (*17*). In Fig. 4B the threshold for appearance of the fullerene fragments (which is nearly identical to the threshold for loss of the polycyclic rings) is compared with the threshold calculated with an activation energy of 2.4 eV. The calculated threshold is significantly sharper than that observed experimentally. Most of this discrepancy probably arises from the presence of a number of different polycyclic ring isomers with slightly different activation energies. From these simulations, we estimate an average activation energy of ~2.4 eV for annealing of the polycyclic rings and ~3.7 eV for annealing the monocyclic ring. These activation energies are sufficiently small that both of these processes may play an important role in the carbon arc synthesis of fullerenes where temperatures have been estimated to be 1000 to 2000 K (*18*). Conversion from the planar polycyclic and monocyclic rings to a closed shell of hexagonal and pentagonal rings must surely represent some of the most dramatic molecular rearrangements in modern chemistry, yet the activation energies for these processes appear to be comparable to the strength of a single C–C bond. The driving force for these structural interconversions is the overwhelming stability of the spheroidal shell, which is clearly demonstrated by the fact that a substantial fraction of the fullerenes generated by annealing of the polycyclic rings are produced sufficiently excited that they subsequently fragment.

We have performed similar studies of other carbon cluster ions containing 50 to 70 atoms and found that the behavior reported here for C_{60}^+ is not unique: for example, annealing of a 58-atom cluster to a spheroidal fullerene occurs almost as easily as for a 60-atom cluster. However, for clusters with fewer than 50 atoms, fullerene formation diminishes sharply as annealing into large monocyclic rings becomes the dominant process. Hence, our studies confirm that coalescence of medium-sized polyyne rings followed by annealing is likely to be an important route in fullerene synthesis. However, while annealing of the polycyclic rings provides a direct route to the large spheroidal fullerenes, this process cannot apparently account for why some specific fullerenes are formed in such large relative abundances (unless the behavior of C_{60} is dramatically different to that of C_{60}^+). After formation of a large spheroidal shell, presumably it is their low reactivity toward small carbon species such as C_2 (6) that is responsible for the preponderance of certain fullerenes. Because formation of a spheroidal fullerene is not unique to C_{60}^+, these results suggest that preparation of a polyyne precursor, followed by photochemical activation in an inert environment, may provide a general route for the synthesis of fullerenes of any size. The challenge now is to determine which of the possible polyyne ring isomers are the best potential precursors.

REFERENCES AND NOTES

1. Q. L. Zhang *et al.*, *J. Phys. Chem.* **90**, 525 (1986); H. Kroto, *Science* **242**, 1139 (1988).
2. T. W. Ebbesen, J. Tabuchi, K. Tanigaki, *Chem. Phys. Lett.* **191**, 336 (1992).
3. A. Goeres and E. Sedlmayr, *ibid.* **184**, 310 (1991); M. Broyer *et al.*, *ibid.* **198**, 128 (1992).
4. T. Wakabayashi and Y. Achiba, *ibid.* **190**, 465 (1992).
5. T.-M. Chang, A. Naim, S. N. Ahmed, G. Goodloe, P. B. Shevlin, *J. Am. Chem. Soc.* **114**, 7603 (1992).
6. J. R. Heath, *ACS Symp. Ser.* **481**, 1 (1991).
7. Y. Rubin, M. Kahr, C. B. Knobler, F. Diederich, C. L. Wilkins, *J. Am. Chem. Soc.* **113**, 495 (1991); S. W. McElvaney, M. M. Ross, N. S. Goroff, F. Diederich, *Science* **259**, 1594 (1993).
8. M. F. Jarrold and V. A. Constant, *Phys. Rev. Lett.* **67**, 2994 (1991); M. F. Jarrold and J. E. Bower, *J. Chem. Phys.* **96**, 9180 (1992).
9. M. F. Jarrold and E. C. Honea, *J. Phys. Chem.* **95**, 9181 (1991); *J. Am. Chem. Soc.* **114**, 459 (1992).
10. G. von Helden, M.-T. Hsu, P. R. Kemper, M. T. Bowers, *J. Chem. Phys.* **95**, 3835 (1991); see also R. M. Baum, *Chem. Eng. News* **70** (no. 22), 25 (1992).
11. J. Hunter, J. Fye, M. F. Jarrold, *J. Phys. Chem.*, in press.
12. E. A. Mason and E. W. McDaniel, *Transport Properties of Ions in Gases* (Wiley, New York, 1988).
13. L. A. Bloomfield, M. E. Geusic, R. R. Freeman, W. L. Brown, *Chem. Phys. Lett.* **121**, 33 (1985); S. C. O'Brien, J. R. Heath, R. F. Curl, R. E. Smalley, *J. Chem. Phys.* **88**, 220 (1988); R. J. Doyle and M. M. Ross, *J. Phys. Chem.* **95**, 4954 (1991).
14. M. E. Geusic, M. F. Jarrold, T. J. McIlrath, R. R. Freeman, W. L. Brown, *J. Chem. Phys.* **86**, 3862 (1987); P. P. Radi, T. L. Bunn, P. R. Kemper, M. E. Molchan, M. T. Bowers, *ibid.* **88**, 2809 (1988).
15. W. Forst, *Theory of Unimolecular Reactions* (Academic, New York, 1973).
16. R. K. Yoo, B. Ruscic, J. Berkowitz, *J. Chem. Phys.* **96**, 911 (1992); P. Wurz and K. R. Lykke, *J. Phys. Chem.* **96**, 10129 (1992); P. Sandler, C. Lifshitz, C. E. Klots, *Chem. Phys. Lett.* **200**, 445 (1992).
17. M. B. Sowa, P. A. Hintz, S. L. Anderson, *J. Chem. Phys.* **95**, 4719 (1991).
18. R. E. Haufler *et al.*, *Mater. Res. Soc. Symp. Proc.* **206**, 627 (1991).

15 January 1993; accepted 6 April 1993

A Photomicrodynamic System with a Mechanical Resonator Monolithically Integrated with Laser Diodes on Gallium Arsenide

Hiroo Ukita, Yuji Uenishi, Hidenao Tanaka

A cantilever resonant microbeam, laser diodes, and a photodiode have been fabricated on the surface of a gallium arsenide substrate. The microbeam is excited photothermally by light from a laser diode. The vibration is detected with a photodiode as the variation in light output caused by the difference in optical length between the microbeam and another laser diode. A high carrier-to-noise ratio (45 decibels) is achieved with a short (3 micrometers) external cavity length. Such a small distance allows a lensless system, which increases the ease of fabrication. This work could lead to applications in which photomicrodynamic systems are monolithically integrated on a gallium arsenide substrate with surface micromachining technology.

Established large-scale integration manufacturing techniques, such as photolithography, can be used for fabricating microstructures including resonant sensors, motors, valves, and pumps (*1–3*). Such microdevices have been made from silicon wafers, which have isodirectional etching properties. However, it has been impossible to integrate a light source with these Si-based micromechanical structures. Gallium arsenide (GaAs), on the other hand, is attractive for integrating optical and mechanical structures. The advantage of using an optical method is that it does not interfere electromagnetically. Furthermore, it could lead to developments in photomicrodynamics. With GaAs, not only would optical sensors and actuators be possible, but also micromechanical filters for optical signal processing and pickups for optical recording (*4, 5*).

A resonant sensor is a device that changes its mechanical resonant frequency as a function of a physical or chemical parameter, such as stress or mass-loading (*6*). Electrostatic (capacitive) excitation and detection or piezoelectric excitation and detection have been used for the conventional Si-based resonant sensors. The former method requires comparatively large electrode areas and small electrode distances (a few micrometers) if good signals are to be obtained. The latter requires a layer of a

NTT Interdisciplinary Research Laboratories, 9-11 Midori-cho 3-Chome, Musashino-shi, Tokyo 180, Japan.